Energy-saving effect of low-cost and environmentally friendly sepiolite as an efficient catalyst carrier for CO2 capture

Journal:	*ACS Sustainable Chemistry & Engineering*
Manuscript ID	sc-2022-06739w.R2
Manuscript Type:	Article
Date Submitted by the Author:	17-Feb-2023
Complete List of Authors:	Zhang, Rui; Xiangtan University, College of Chemical Engineering Li, Yufan; Xiangtan University Zhang, Yiming; Xiangtan University Li, Ting; Xiangtan University Yang, Luning; Xiangtan University LI, Chao'en; Commonwealth Scientific and Industrial Research Organisation, Energy Barzagli, Francesco; Istituto di chimica dei composti organo metallici Zhang, Zhien; Ohio State University, William G. Lowrie Department of Chemical and Biomolecular Engineering; West Virginia University

Energy-saving effect of low-cost and environmentally friendly sepiolite as an efficient catalyst carrier for CO_2 capture

Rui Zhang[1]*, Yufan Li[1], Yiming Zhang[1], Ting Li[1], Luning Yang[1], Chao'en Li[2], Francesco Barzagli[3]*, Zhien Zhang[4]*

[1] College of Chemical Engineering, Xiangtan University, Xiangtan, Hunan 411105, P.R. China.

[2] CSIRO Energy, 71 Normanby Road, Clayton North, Victoria 3169, Australia.

[3] ICCOM Institute, National Research Council, via Madonna del Piano 10, 50019 Sesto Fiorentino, Florence, Italy

[4] William G. Lowrie Department of Chemical and Biomolecular Engineering, The Ohio State University, Columbus, OH 43210, USA.

*Corresponding Authors:

1. Dr. Rui Zhang, Email: ruizhang@xtu.edu.cn, tange1026@163.com
2. Dr. Zhien Zhang: Email: zhienzhang@hotmail.com, zhang.4528@osu.edu
3. Dr. Francesco Barzagli, Email: francesco.barzagli@iccom.cnr.it

ABSTRACT

Recently, the development of efficient solid acid catalysts to promote CO_2 desorption rate while reducing energy consumption has attracted much attention. In this work, the low-cost environmentally friendly Sepiolite (SEP) clay was evaluated as a support of metal oxides (Fe_2O_3, CuO) catalysts. By comparing their catalytic performances for CO_2 desorption from the CO_2-rich monoethanolamine (MEA) solution at 100℃, the obtained results showed that the tested catalysts could accelerate the CO_2 release rate and reduce the heat consumption in comparison with non-catalytic MEA solution. The relative heat duty found decreased in the order: blank (100%) > SEP (66.4%) > CuO-SEP (58.8%) > Fe_2O_3-SEP (54.0%). Recycling tests to study stability demonstrated that Fe_2O_3-SEP could maintain its catalytic efficiency after 6 recycling runs. Characterization studies revealed that a high mesoporous specific surface area and a high ratio of Brønsted and Lewis acid sites are beneficial to enhance the activity of the catalysts. In addition, a possible catalytic mechanism for CO_2 desorption was proposed. As a result, this work proved that sepiolite has the potential to be a low-cost and competitive catalysts carrier for CO_2 capture.

Keywords: carbon capture, monoethanolamine, heat consumption, catalysts, sepiolite, catalytic mechanism

Synopsis sentence： The sepiolite could be used as a competitive catalyst carrier to prepare the efficient catalyst for CO_2 desorption.

■ Introduction

Carbon dioxide (CO_2) has been accused as one of major responsible contributors for the increasingly serious climate problem due to the raising concentration of CO_2 in atmosphere[1]. CO_2 capture technology has been investigated widely for controlling CO_2 emissions from industrial flue gas, and the amine-based chemical absorption process has been regarded as the most mature method for the post-combustion CO_2 capture [1, 2]. However, the large-scale application of amine-based CO_2 capture technology is still challenging, mainly because of the huge heat requirement in the amine solvent regeneration process (CO_2 desorption) [3, 4]. Many efforts have been made to overcome the drawbacks of the amine-based CO_2 capture technology including the development of new absorbents and the use of other new technologies for enhancing the CO_2 capture efficiency [5-11]. It was reported that the heat cost for solvent regeneration contributes more than 70% of the total heat cost, which constrains the industrial application of this technology [3, 12].

The heat consumption in the solvent regeneration process consists of reaction heat, evaporations heat, and sensible heat [12]. To regenerate the amine solvent, the traditional method involves supplying heat to release CO_2 from the CO_2-species, namely carbamate and bicarbonate/carbonate, by breaking the C-N and C-O bonds, respectively. On the other hand, it is also necessary to supply heat for the endothermic deprotonation of the protonated amine. The heat requirement to restore the amine determines that the

solvent regeneration (CO_2 desorption) process must be performed at a high desorption temperature, normally at 120-140℃ [13]. High temperature results in high energy consumption. Moreover, the high desorption temperature causes degradation of the absorbent, and then the CO_2 capture efficiency is expected decreasing after a long running period.

Recently, solid acid catalysts aided CO_2 desorption process have attracted much attentions aiming to minimize the energy consumption of the process[14-18]: the addition of solid acid catalysts allows the CO_2 desorption process to be performed at a relative low temperature (below 100℃), which not only accelerates the CO_2 desorption rate but also decreases the heat consumption for releasing CO_2. It is commonly accepted that the main contributor for the high heat consumption during the CO_2 desorption are the carbamate decomposition and deprotonation of protonated amine, and both processes involve proton transfer [13, 19]. Solid acid catalysts can promote two reaction process above mentioned because of their remarkable acidity and the presence of Brønsted and Lewis acid sites[20]. Liang et al.[21] reported that the solid catalyst HZSM-5 (Brønsted acid dominated) and γ-Al_2O_3 (Lewis acid dominated) could reduce the heat duty efficiently in the commercial aqueous Monoethanolamine (MEA) solution regeneration process. Recently, Bhatti et al. [22] investigated several metal oxides catalysts to improve CO_2 desorption performance in a nonaqueous 2-(2-aminoethoxy)ethanolamine (DGA) solution at the desorption temperature of 90°C; as a result, WO_3 and TiO_2 showed remarkable advantages in enhancing the CO_2 desorption performance. Zhang et al. [23]

studied SAPO-34 and SO_4^{2-}/TiO_2 for the catalytic CO_2 desorption from CO_2 loaded MEA solution under the relative low temperature of 96 ℃, their results revealed that the Brϕnsted/Lewis acid sites on the catalysts are beneficial to the $MEAH^+$ deprotonation and carbamate decomposition, and a high mesopore surface area (MSA) also enhances the catalytic CO_2 desorption performance. Zhang et al. [19] loaded several metal oxides, namely CuO, Fe_2O_3 and NiO, over KIT-6 to prepare new catalysts for CO_2 desorption, and a remarkable decrease in the heat consumption (by 33.4%) was observed when CuO-KIT-6 was used, which confirmed that MSA is an important indicator for improving the catalytic performance. In addition, Xing et al.[24] selected SO_4^{2-}/ZrO_2 as active component loaded on HZSM-5 catalyst to improve the Brϕnsted/Lewis acid sites, and their results showed that the desorption rate was increased significantly with the aid of the SO_4^{2-}/ZrO_2-HZSM-5 catalyst in comparison with the non-catalytic process. Furthermore, the heat consumption in the solvent regeneration process decreased up to 30% as well.

However, with different catalyst carriers, the same catalyst, for example, SO_4^{2-}/ZrO_2, shows different catalytic performances [24-28]. Unfortunately, the current reported catalyst carriers were normally synthesized using complicated, cost expensive, and environmentally unfriendly preparation methods, which prohibits the large-scale application of catalytic CO_2 desorption technology. Therefore, finding a stable, environmentally friendly carrier with a proper pore structure could be very helpful to promote the catalytic CO_2 desorption process.

Recently, natural clay materials have raised the interest of scientists because of their competitive porous properties, low-cost, easy acquirement, and environment friendliness, and have been widely used for the preparation of adsorption materials and catalysts [29-32]. Tan et al. [13] investigated attapulgite (ATP) as a cost-effective catalyst to catalyze the CO_2 desorption, capable of increasing CO_2 desorption rate by 54-57% while reducing the heat duty by 32%. Bhatti et al. [32] exploited different acids to activate the montmorillonite (Mont) and used them to catalyze CO_2 desorption. They found that all acid-activated montmorillonite catalysts showed high catalytic activity, especially the H_3PO_4 activated montmorillonite catalyst (PO_4-Mont) was able to reduce the heat duty by 32.4% and increase the desorption rate by 75%. Moreover, Bhatti modified montmorillonite via ion-exchange using H_2SO_4 and Zr was able to improve the CO_2 desorption rate by up to 215% and reduce the heat duty by up to 44.15% [31]. Bhatti et al. [33] further used Fe and Co to enhance the catalytic activity of montmorillonite, achieving a 315% increase in CO_2 desorption and a 40% decrease in heat duty. In addition, the work of Tan et al.[34] further indicates that the metal oxides can enhance the catalytic CO_2 desorption performance of attapulgite in terms of the amount of desorbed CO_2 and heat duty. It is noteworthy that all studied clay-based catalysts demonstrated prominent stability after the recycling experiments in the laboratory test.

Sepiolite (SEP, $Si_{12}O_{30}Mg_8(OH)_4(H_2O)_4 \cdot 8H_2O$) as one of the clay minerals has the similar layered structure with montmorillonite, however, it has insufficient octahedral sheets in comparison with the later [35]. Sepiolite is a pure trioctahedral mineral in the

form of two-dimensional tetrahedral sheet of SiO_5 [36-38]. The platelet edges on SEP structure normally have a few positive charges that could stretch the species with negative charges. Meanwhile, the -OH and anionic groups on the SEP surface could participate in chemical reactions and extend the crystal interlayer spacing [38]. **Figure 1** shows the schematic structure of SEP: due to the presence of the cations and the three kinds of water in the structure, SEP could have both Brønsted and Lewis acid sites available when it reacts with other species. These peculiarities might have potential to promote the CO_2 desorption process. Furthermore, more works have proved that the metal oxides could further improve the CO_2 desorption performance of the catalyst carrier[13, 39, 40]. In addition, when the surface of the metal oxide is exposed to water, more acidic Brønsted (-OH) sites can be generated, which promote the $MEACOO^-$ decomposition[39]. Hence, since SEP is a natural clay mineral and an easy material to obtain, it is worth to be investigated when it is used as a catalyst carrier to combine with metal oxides in CO_2 desorption process in terms of the CO_2 desorption rate, the amount of desorbed CO_2, and the heat consumption.

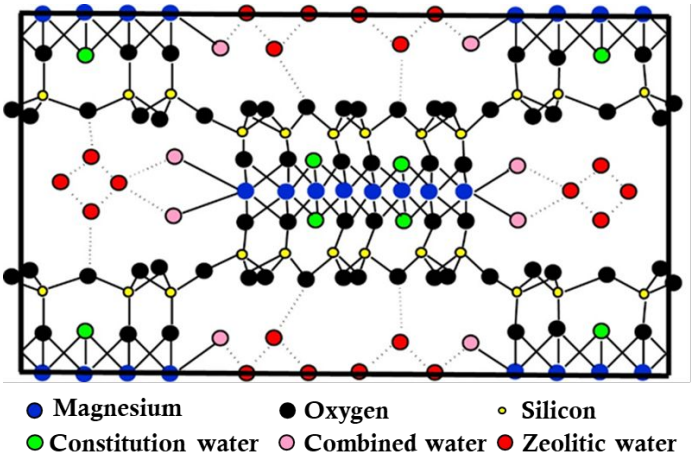

Figure 1. A schematic structure of Sepiolite (SEP).

■ Experimental Section

Chemicals

High or ultra-high purity gases used in this work including carbon dioxide (CO_2, 99.999%) and nitrogen (N_2, 99.9%) were acquired from Hunan Zhongtai Hongyuan Gas Co., Ltd. The materials used for the catalyst preparation including iron (III) nitrate nonahydrate ($Fe(NO_3)_3 \cdot 9H_2O$, 98.5%), copper nitrate trihydrate ($Cu(NO_3)_2 \cdot 3H_2O$, 99%), as well as monoethanolamine (MEA, 99%), were purchased from Shanghai Macleans Biochemical Co., Ltd., while the sepiolite (SEP) was acquired from Hunan Lihengtong New Material Co., Ltd. All chemicals were used without further purification in this work.

Catalyst preparation

The impregnation method was used to prepare the catalysts in this work. Certain amount of $Fe(NO_3)_3 \cdot 9H_2O$ with the purity of 98.5% and SEP (each with 3 grams) was firstly immersed in deionized water (100 mL) and then was stirred with a magnetic stirring bar at 900 revolutions per minute (rpm) for 12 hours at the temperature of 40 ℃ until the solid chemicals dissolved completely. Secondly, the prepared solution was heated up to 80 ℃ for 4 hours to evaporate most of the free water. The wet sample then was dried at 100 ℃ for 8 hours in a drying oven. Lastly, the sample was calcinated at 550 ℃ for 5 hours. The desired catalyst, Fe_2O_3-sepiolite (Fe_2O_3-SEP), was finally obtained. The same method was used to synthesize the CuO-sepiolite catalyst (CuO-

SEP) in this work as well. More details for the preparation procedure of catalysts were also reported in our previous published work [19]. In addition, different techniques were used in this work to characterize the physicochemical properties of prepared catalysts; details can be found in our previous study, and the same method was also applied in this work[19].

Experimental measurement

In this work, 200 mL of 5M aqueous MEA solution was used to prepare the CO_2 rich MEA solution by using the experimental set-up described in the work of Zhang et al.[19]: the CO_2 absorption process was performed at 40 ℃ with a CO_2 partial pressure of 100kPa. The final CO_2 loading was determined by using the titration method with 1M HCl solution [41], and the obtained results indicated that the CO_2-rich loading was 0.590 mol CO_2/mol amine. Then the prepared CO_2 rich MEA solution was used for all the CO_2 desorption experiments to evaluate the catalytic performance of the synthesized catalysts, and the scheme for experimental set-up also can be found in our previous published work[19]. Desorption experiments were conducted on 200 mL of solution, with and without the catalysts, so as to have a reference under the same operating conditions (blank). In the catalyst-aided desorption experiments, 2.5 grams of catalyst was put into the three-necked flask reactor containing the CO_2-rich MEA solution (the mass ratio of catalyst to amine solution is 1.25:100). Desorption experiments were performed at the temperature of 100 ℃ with an oil bath, which was covered with insulating cotton (with a thickness of about 5 cm) to avoid the effect of room temperature. The desorbed CO_2

was carried a the pure N_2 gas stream (500mL/min) and its concentration was analyzed with an infrared CO_2 analyzer (COZIR-100, ± 0.01% in accuracy, GSS Ltd., UK) and recorded by computer with an interval time of 10 seconds. Here the CO_2 loading in the liquid gas can be calculated based the obtained CO_2 concentration in the outlet gas at each record time, the details for the calculation method can be found in the work of Zhang et al.[41].

In addition, to better understand the reaction mechanism, the speciation for the CO_2 loaded MEA solution at different CO_2 loading were analyzed by using a Nuclear Magnetic Resonance (NMR) spectrometer (Bruker Avance III 400) at the temperature of 25 ℃. The NMR analysis conditions and sample preparation method involved in this work were the same as those used and validated in our previous work[42].

Parameters for evaluating the catalytic performance

To evaluate and compare the catalytic CO_2 desorption performances of the synthesized catalysts, a series of parameters such as CO_2 desorption rate (V_d, mol-CO_2/mol-amine/min), CO_2 desorption capacity (n, mole) and heat duty (H, kJ/mol-CO_2) were selected and calculated as shown in Equations 1-3, respectively:[19].

$$V_{\mathrm{d}} = \frac{\frac{V_{\mathrm{N_2}} \times \mathrm{C}'}{1-\mathrm{C}'} \times \frac{273.15}{V_{\mathrm{m}} \times T}}{C \times V} \quad (1)$$

$$\mathrm{n}_{CO_2} = (\alpha_{rich} - \alpha_{lean}) \times V \quad (2)$$

$$H = \frac{\text{Heat input/time}}{\mathrm{CO_2}\text{ amount/time}} = \frac{\mathrm{E(kJ)}}{n_{CO_2}(mol)} \quad (3)$$

where the V_{N_2} is the flow rate of the carrier gas, N_2; C' is the concentration of CO_2 in the exit gas mixture, mol%; V_m is the standard molar volume of gases, 22.4 L/mol; T is the room temperature, K; C is the concentration of the MEA solution, 5 mol/L; V is the volume of the MEA solution in the reactor, 0.2 L; α_{rich} is the CO_2-rich loading in mol-CO_2/mol-amine; α_{lean} is the CO_2-lean loading in mol-CO_2/mol-amine; and E is the recorded electricity consumption, kJ; n_{CO_2} is the CO_2 desorption capacity in moles.

The heat duty (Equation 3) measured in this work is defined as the heat required for the release of one mole of CO_2, and it can be described by the ratio between the heat input and the amount of desorbed CO_2 using a widely accepted approach[24, 43-45]. In this work, heat consumption for sorbent regeneration was reported as electricity consumption measured using a digital electric meter (Zhejiang Tepsung Electric Co., Ltd.) for the entire duration of the desorption process; this method, commonly used in laboratory-scale testing, allows for a reasonable relative comparison to evaluate the catalytic performance of different catalysts in a single work for each parallel test.

It should be noted, however, that the obtained values of these parameters can only be used in this work for comparison purposes, since a relatively low temperature was applied in this work to provide a relatively slow CO_2 desorption rate which could amplify the differences between the various catalytic systems.

The relative desorption energy consumption (RH, Equation 4) was also used to compare the catalytic performances of the catalysts studied in this work [46]. In addition,

the desorption factor (DF, $mol^3/(kJ \cdot min)$) was adopted to further correlate the structure-activity relationship between the catalyst and the CO_2 desorption performance, as shown in Equation 5 [19]:

$$\mathrm{RH}(\%) = \frac{H_\mathrm{i}}{H_0} \times 100 \quad (4)$$

$$\mathrm{DF} = \frac{V_\mathrm{d} \times \mathrm{n}co_2}{H_\mathrm{i}} \quad (5)$$

where H_i and H_0 are the heat duty in the solvent regeneration process with and without catalyst, respectively.

■ Results and Discussion

Evaluation of the desorption performance of the catalyst

In this work, the catalytic CO_2 desorption performances of Fe_2O_3-SEP and CuO-SEP in CO_2-loaded MEA solutions were investigated by determining the desorption rate, desorption capacity, and relative energy consumption during regeneration processes conducted at 100°C with a mass ratio of catalyst to amine solution of 1.25:100. **Figure 2** displays the changes in the relative CO_2 loadings in the amine solution with and without catalysts. It clearly shows that the CO_2 remained in the MEA solution decreases rapidly at the desorption time between 10 and 30 minutes. The final CO_2 loadings for all systems are almost the same, indicating that the CO_2 desorption processes finally reach an equilibrium state. This also demonstrates that the addition of catalyst can only accelerate the CO_2 desorption rate, but not change the chemical equilibrium of the desorption reaction.

Figure 2 also demonstrates that the CO_2 desorption starts earlier with all tested catalysts than with the non-catalytic MEA solution (blank). The activity for CO_2 releasing decreases in the order Fe_2O_3-SEP > CuO-SEP > SEP > blank. The metal oxides loaded on the SEP carrier might behave as an active site to catalyze the CO_2 desorption, and the Fe_2O_3-SEP catalyst performs better than others tested in this work.

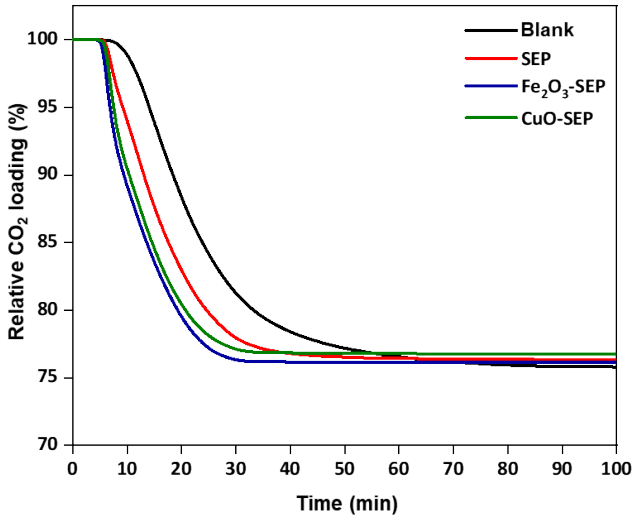

Figure 2. Comparison of CO_2 releasing rates with and without catalyst.

As mentioned in our previous works [13, 19], the CO_2 desorption performance can be assessed by the CO_2 desorption rate, the amount of desorbed CO_2 and the energy consumption, calculated from the data acquired in the first 20 minutes of the desorption experiments, because the CO_2 loading drops rapidly in the first 10-30 minutes during the CO_2 desorption process and then slows down as shown in **Figure 2**. **Figure 3** illustrates the desorption performances in different CO_2 loaded MEA solutions with and without catalysts, in terms of average CO_2 desorption rate, desorption capacity and relative desorption energy consumption. The results showed that the average CO_2 desorption rate ($\times 10^{-4}$ mol/min) decreased in the order Fe_2O_3-SEP (62.9) > CuO-SEP

(59.4) > SEP (51.2) > blank (34.9), and the same trend was also found for the CO_2 desorption capacity ($\times 10^{-2}$ mol), i.e. Fe_2O_3-SEP (12.6) > CuO-SEP (11.9) > SEP (10.2) > blank (7.0). In contrast, the relative desorption energy consumption RH (%) followed the order blank (100) > SEP (66.4) > CuO-SEP (58.8) > Fe_2O_3-SEP (54.0). **Figure 3** shows that, for MEA system, the addition of catalyst can accelerate the CO_2 desorption rate by 46.7-166.2 %, increase the CO_2 desorption capacity by 45.7-80.0 %, and reduce the energy demand by 33.6 -46.0 %. Therefore, the CO_2 desorption efficiency in the MEA regeneration process can be significantly improved with the addition of SEP-based catalysts, among which the best results can be obtained with Fe_2O_3-SEP.

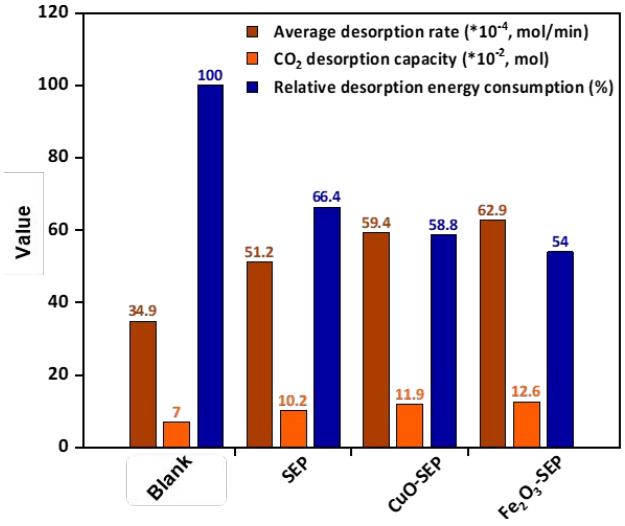

Figure 3. Comparison of the CO_2 desorption performances of SEP-based catalysts.

Table 1 illustrates a comparison of the catalytic CO_2 desorption performance between the catalysts prepared in this work and others reported in the literature. The reported desorption performance data refer to the use of the indicated catalyst in CO_2-loaded solutions of MEA 5M. As evident, the use of solid acid catalysts generally results in an increase in the amount of CO_2 desorbed (values greater than 0%) and a

decrease in Relative heat duty (percentages less than 100%) compared to 5M MEA desorbed in the absence of any catalyst. It is worth noting that all experimental data reported in **Table 1** refer to a desorption temperature ≤ 100 °C, which is significantly lower than that of the conventional process (120-140 °C): this lower temperature, which is possible precisely because of the use of catalysts, helps to effectively reduce the heat of evaporation for solvent regeneration and thus promote the reduction of the heat duty.

Although the catalytic desorption performances were determined under conditions that were not always homogeneous with each other (due to different dosage of the catalysts used, desorption temperature, stirring or total desorption time), the comparison shown in **Table 1** highlights the potential advantages of SEP-based catalysts: their high performance, combined with important features such as low cost and environmental compatibility, indicating that SEP-based catalysts are deserved to be further studied in the future. In particular, the enormous reduction in energy consumption for solvent regeneration achieved in this work for CuO-SEP and Fe_2O_3-SEP catalysts could significantly reduce the operating cost, further encouraging the industrial application of amine-based carbon capture technology.

Table 1. CO_2 catalytic desorption performance of different catalysts when added to CO_2-loaded 5M MEA solution. Percentages refer to increases or decreases from values obtained under the same operating conditions by desorbing MEA without using catalysts

Catalysts	Desorption temperature (℃)	Increase in desorbed CO_2 amount (%)	Relative heat duty (%)	Reference
SEP	100	46	66.4	This work
CuO-SEP	100	70	58.8	
Fe_2O_3-SEP	100	80	54	
KIT-6	100	31	79.8	33
Cr-Mont	86	26.2	79.1	
Co-Mont	86	45.5	67.6	
Fe-Mont	86	82.4	60	
CuO-KIT-6	100	49	66.6	19
NiO-KIT-6	100	32	75.4	
Fe_2O_3-KIT-6	100	34	76.5	
SO_4^{2-}/ ZIF-67-C@TiO_2	88	65	64	16
SO_3H-MCM-41	90	53	68	44
Al_2O_3-HZSM-5	96	38	66	47
SO_4^{2-}/ZrO_2-Al_2O_3	98	34	62	28
SO_4^{2-}/ZrO_2-SiO_2	97	40	64	27
CMK-3-SBA-15	97	6.9	78.5	48
CMK-3-MCM-41	97	17.2	69.7	
CMK-3-SiO_2	97	69	62.6	
Ce-M-HPW-15	88	38.1	70.5	49

SAPO-34	96	28.1	75.7	[23]
SO_4^{2-}/ZrO_2-HZSM-5	98	40	69	[24]

Catalyst characterization and structure-activity relationship

Figure 4 presents the wide-angle XRD patterns of three catalysts (SEP, Fe_2O_3-SEP, CuO-SEP) in the range of 5 to 90°. The characteristic diffraction peaks of SEP usually appear at 7.2, 20.6, 26.5, 27.9, 35.0, and 39.9°, respectively [50]. It can be observed that the main characteristic peaks of all samples did not change significantly compared to SEP-carrier, which indicates that the samples still retain their original crystal structure after loading metal oxides. The characteristic diffraction peaks of Fe_2O_3-SEP at 35.6, 40.8, 54.1, 62.3, and 63.8° correspond to α-Fe_2O_3 [51, 52]. CuO-SEP generates characteristic diffraction peaks at 35.5, 38.6, 48.6, 62.4, and 66.2°, respectively [53]. These profiles demonstrate that the metal oxides were loaded on SEP-carrier successfully and without affecting the crystal structure of SEP.

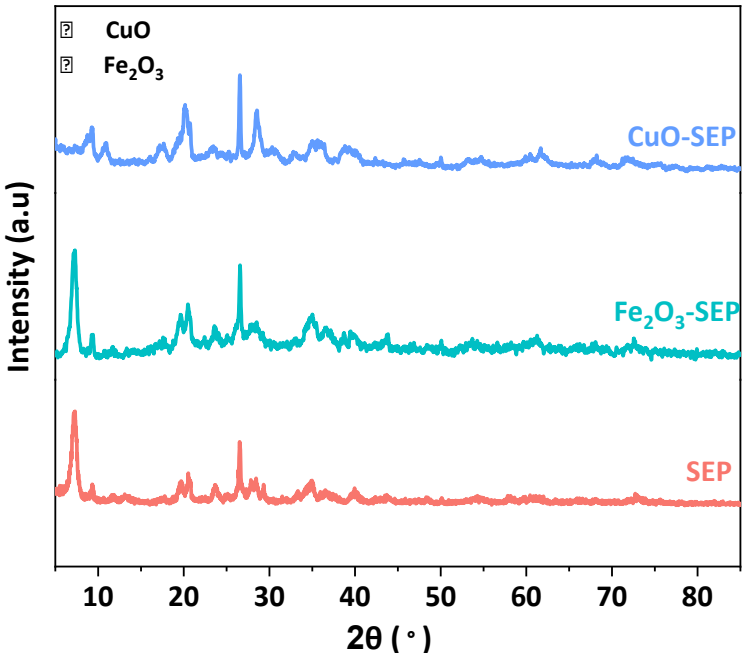

Figure 4. X-ray diffractograms of SEP-based catalysts.

The FT-IR spectra of the three SEP-based catalysts are shown in **Figure 5**. It can be observed that the three catalysts show similar IR spectra, with absorption peaks at 3348 and 1654 cm^{-1} attributable to the stretching vibration of the hydroxyl group in SEP, which is caused by the presence of zeolite and combined water, respectively, in the SEP structure. The characteristic absorption peaks at 1027 and 469 cm^{-1} are caused by the antisymmetric stretching vibration of Si-O bond and the bending vibration of Si-O-Si bond on SEP tetrahedral silicon wafer [54, 55]. The absorption peak at 1027 cm^{-1} is still present after loading metal oxides, which proves that the basic structure of SEP has not changed. The decreased width of absorption peaks at 3348 and 1027 cm^{-1} indicates the presence of metal oxides in SEP structure, while the appearance of new absorption peaks at 3752 and 899 cm^{-1} indicates the presence of new substances in SEP. FT-IR results show that part of the structure of SEP was retained and the metal oxides were

completely dispersed on the surface or skeleton of SEP. Based on the obtained characteristic results, it can be concluded that Fe_2O_3-SEP catalyst retains the best SEP structure, in great agreement with the XRD results.

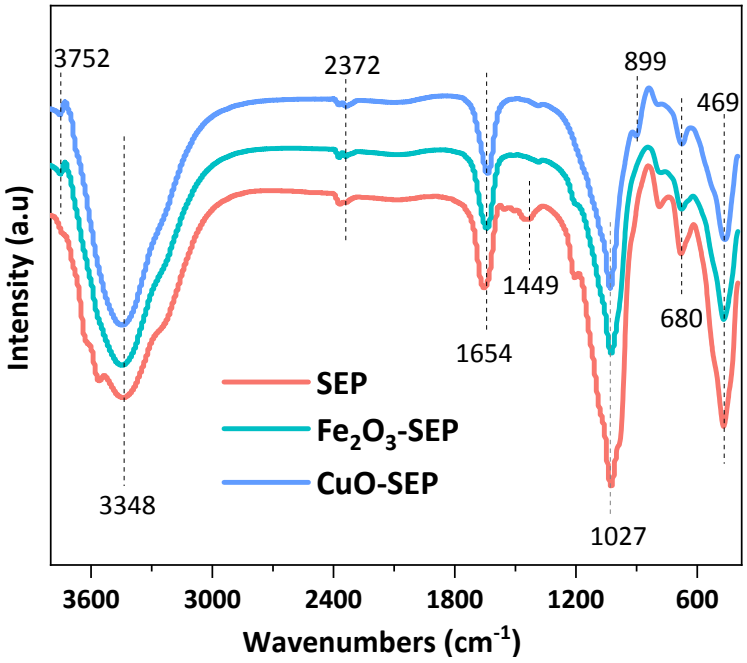

Figure 5. FT-IR spectra of SEP-based catalysts.

The adsorption-desorption isotherms and the BET specific surface area of SEP can be obtained by N_2 adsorption-desorption experiments to analyze the internal changes of SEP before and after metal oxides loading. **Figure 6** presents that N_2 adsorption-desorption curves of supported SEP catalysts belong to class IV adsorption-desorption isotherm with type H3 hysteresis loop according to the catalyst classification prescribed by International Union of Pure and Applied Chemistry (IUPAC). This indicates that all catalysts in the **Figure 6** contain slit-like pore structures. The isotherms of the three catalysts with little differences suggests that SEP retains its original structure after loading metal oxides, which is consistent with the results of XRD and FT-IR.

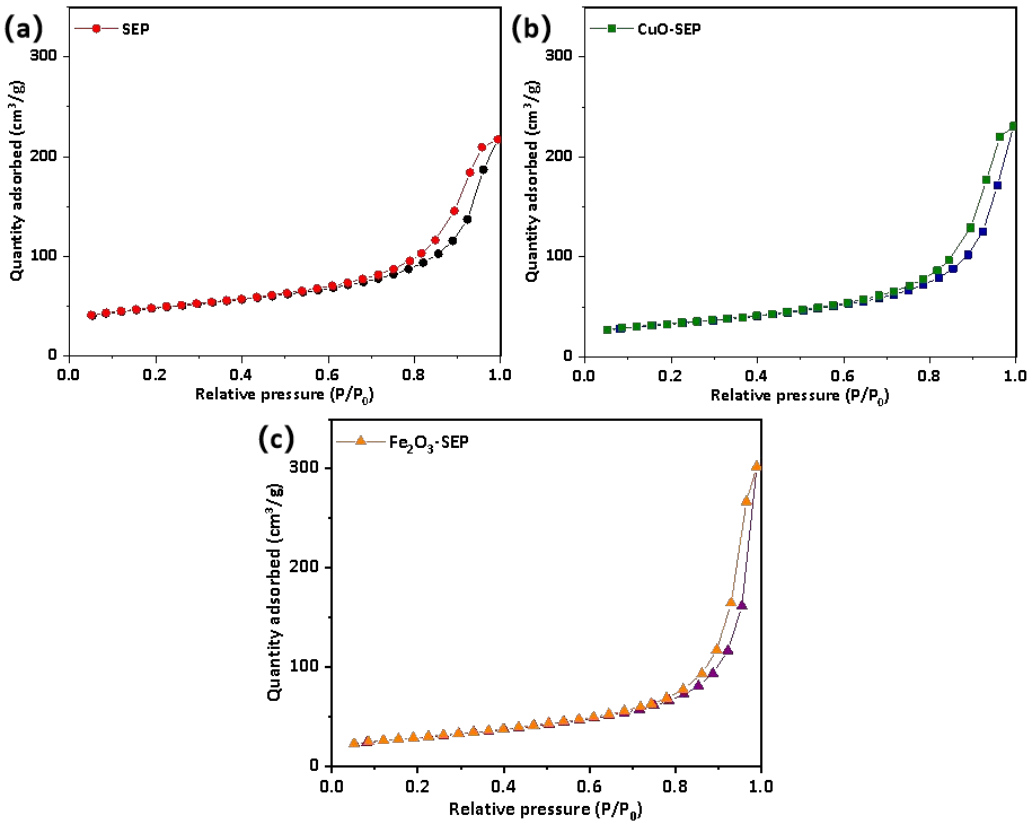

Figure 6. N_2 adsorption - desorption curves for the catalysts of (a) SEP, (b) CuO-SEP and (c) Fe_2O_3-SEP.

The structure and physical properties of the three SEP catalysts are listed in **Table 2**, including the BET specific surface area, pore volume, and pore size. The intermediary pore area was calculated as the BET surface area minus the t-plot micropore area. It can be observed that the specific surface area and pore volume of SEP decrease with the load of metal oxides, but the pore size increases after the load, which may be caused by calcination at high temperature. The mesoporous surface area (MSA) of the three catalysts decreases in the order SEP > Fe_2O_3-SEP > CuO-SEP. A higher MSA and a larger pore size allow more acid sites (Brønsted and Lewis acid) to

be exposed to ions in CO_2 rich solution, especially $MEAH^+$ and $MEACOO^-$, and the interaction between the acid sites and each ion increases to the benefit of the CO_2 desorption process.

Table 2. Structure and physical properties of SEP-based catalysts.

Catalyst	Specific surface area(m^2/g)			Pore volume(cm^3/g)	Pore size(nm)
	Sum	Mesoporous	Microporous		
SEP	159.2	101	58.2	0.27	11.8
CuO-SEP	112.4	86.5	25.9	0.25	14.4
Fe_2O_3-SEP	101.0	90	11.0	0.22	19.2

Pyridine infrared spectroscopy (Py-IR) spectra of the tested catalysts are shown in **Figure 7**. The characteristic absorption peaks of Py-IR spectra at 1540 and 1450 cm^{-1} represent Brønsted and Lewis acid sites, respectively. The intensity of the peak at 1540 cm^{-1} is smaller, indicating that the content of Brønsted acid sites in SEP catalyst is lower. The concentrations of Brønsted and Lewis acid sites as well as the B/L ratios are summarized in **Table 3**. It can be observed that the Brønsted acid content of the three catalysts follows the order Fe_2O_3-SEP > CuO-SEP > SEP, while the Lewis acid contents in the order SEP > CuO-SEP > Fe_2O_3-SEP. In addition, the ratio of Brønsted and Lewis acid sites (B/L) decreases in the order Fe_2O_3-SEP > CuO-SEP > SEP. It has been revealed that more Brønsted acid sites and a higher B/L ratio benefit the catalytic performance for CO_2 desorption[19], which is in agreement with the CO_2 desorption

performances showed in **Figure 3**. Since Fe_2O_3 supported on SEP has a higher content of Brønsted acid site and B/L ratio than the CuO, it should be more competitive in CO_2 desorption process.

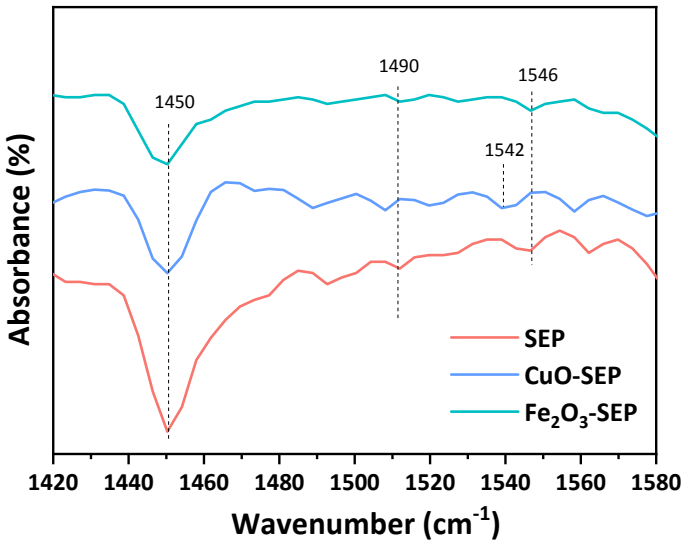

Figure 7. Py-IR profiles of SEP-based catalysts.

Table 3. Acidity analysis of SEP-based catalysts.

Catalyst	Brønsted acid site (mmol/g)	Lewis acid site (mmol/g)	B/L ratio
SEP	0.04	0.90	0.05
CuO-SEP	0.06	0.53	0.12
Fe_2O_3-SEP	0.08	0.36	0.23

For the catalytic CO_2 desorption process, the physical and chemical properties of the catalyst affect its catalytic performance, such as the CO_2 desorption rate, the amount of desorbed CO_2 and the heat duty. The desorption factor (DF), as an evaluating parameter as defined in Equation 5, has been widely used to simply compare the CO_2

desorption performance in different amine systems with and without catalysts: [23, 46], a higher value of DF indicates a better CO_2 desorption performance. To further understand the catalytic performance of SEP-based catalysts for CO_2 release, the desorption factor DF ($mol^3/(kJ \cdot min)$) was correlated with physicochemical properties (MSA, Brønsted acid site content, B/L ratio, etc.), as shown in **Figure 8**. As displayed from **Figure 8a**, even though MSA decreased after loading metal oxides on SEP, the catalytic CO_2 performance of metal oxide supported SEP was enhanced, confirming that the metal oxides improved the catalytic activity of single SEP catalyst. Among the metal oxides modified SEP catalysts, the Fe_2O_3-SEP demonstrates a larger MSA and a better catalytic performance than the CuO-SEP, which means that a larger MSA of the metal oxide modified SEP catalyst is beneficial to improve the catalytic performance for CO_2 desorption. In addition, as observed from the **Figure 8b and 8c**, the catalytic CO_2 desorption performances of the catalysts increase with the Brønsted acid site content and B/L ratio, i.e., the more Brønsted acid sites, the better the catalytic performance. This may be contributed by two characteristics of the catalyst.: A larger MSA allows the acidic Brønsted and Lewis sites to be more easily reached by ions from the CO_2 rich solution. Moreover, the Brønsted acid site (SEP-OH) not only contributes to transfer its own proton to HCO_3^- and $MEACOO^-$ to release CO_2, but also its conjugate base ($SEP\text{-}O^-$) could act as a proton carrier from $MEAH^+$ to $MEACOO^-$ to promote the $MEAH^+$ deprotonation, both of the above behaviors cause the Brønsted acid site to play an important role in the catalytic CO_2 desorption process.

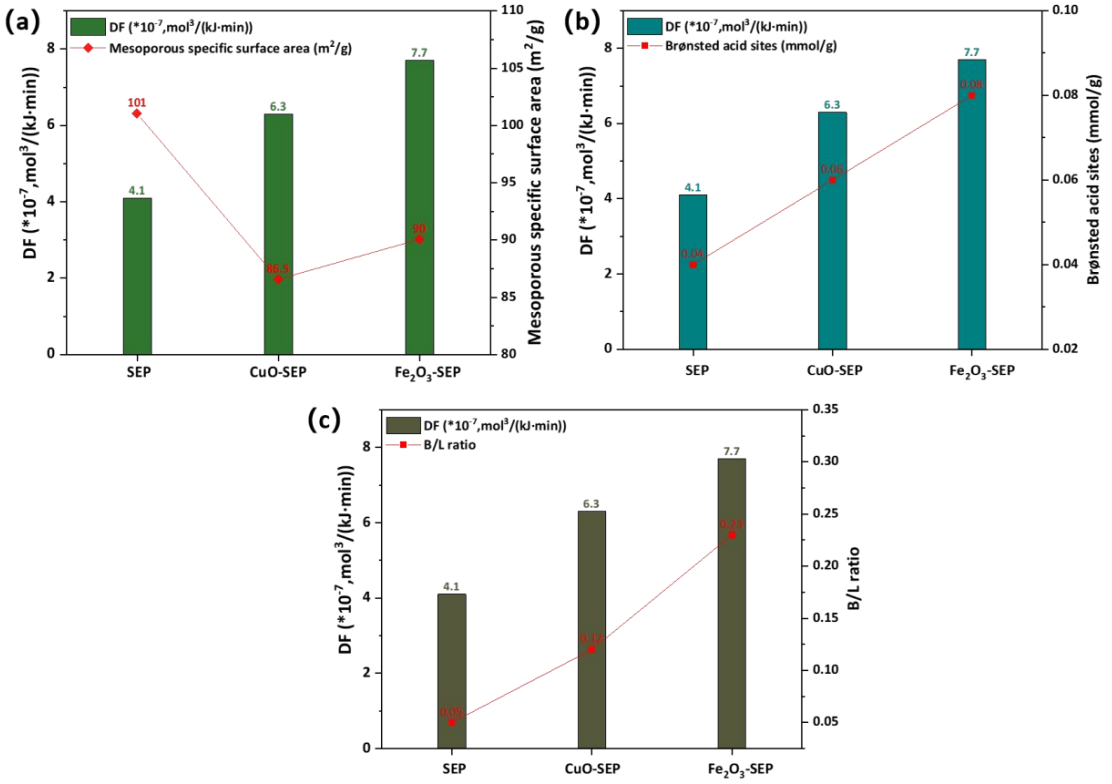

Figure 8. Relationship between the DF and physicochemical properties of catalysts including (a) mesoporous specific surface area, (b) content of Brønsted acid sites and (c) B/L ratio.

Catalytic desorption mechanism

As reported in many published works [14, 15, 23, 46], the regeneration process of MEA solution (CO_2 desorption) includes the decomposition of carbamate (breakdown of N-C bond) and the deprotonation of protonated amine ($MEAH^+$) [56]. The high energy requirement in solvent regeneration is mainly caused by the deprotonation of $MEAH^+$, as the CO_2 loaded amine solution still presents an alkaline environment with lack of H^+. This reaction is therefore endothermic, that is, it requires an external heat input.

In this work, the chemical species present in solution at different CO_2 loadings were identified and quantified by using the ^{13}C NMR technique[57], and the results are plotted in **Figure 9**. Consistent with the literature and our previous studies, $MEAH^+$, $MEACOO^-$, and HCO_3^- are the dominant species at high CO_2 loading (> 0.5) [58, 59]. At the very beginning of the CO_2 desorption process, HCO_3^- acts as a catalyst to obtain H^+ from the $MEAH^+$ and then form H_2CO_3 (**R1**); in addition, the HCO_3^- can also subtract the proton from the hydroxyl group (SEP-OH) on the layered structure of the SEP-based catalyst (**R2**) to form the H_2CO_3 and the conjugated base ($SEP\text{-}O^-$), which in turn accelerate the deprotonation of $MEAH^+$ **(R3)**. This proton transformation process can complete the $MEAH^+$ deprotonation reaction and release CO_2 via the decomposition of H_2CO_3 by heating (**R4**) as the HCO_3^- is not stable when it is heated at the temperature of 100℃. On the other hand, the work of Shi et al. [43] proved that more heat is required for breaking the C-N bond of carbamate than for breaking the C-O bond of HCO_3^- to release CO_2. As a result, the HCO_3^- is consumed quickly at the early stage of the CO_2 desorption.

$$MEAH^+ + HCO_3^- \rightarrow MEA + H_2CO_3 \quad (\mathbf{R1})$$

$$SEP\text{-}OH + HCO_3^- \rightarrow SEP\text{-}O^- + H_2CO_3 \quad (\mathbf{R2})$$

$$SEP\text{-}O^- + MEAH^+ \rightarrow MEA + SEP\text{-}OH \quad (\mathbf{R3})$$

$$H_2CO_3 \rightarrow CO_2 + H_2O \quad (\mathbf{R4})$$

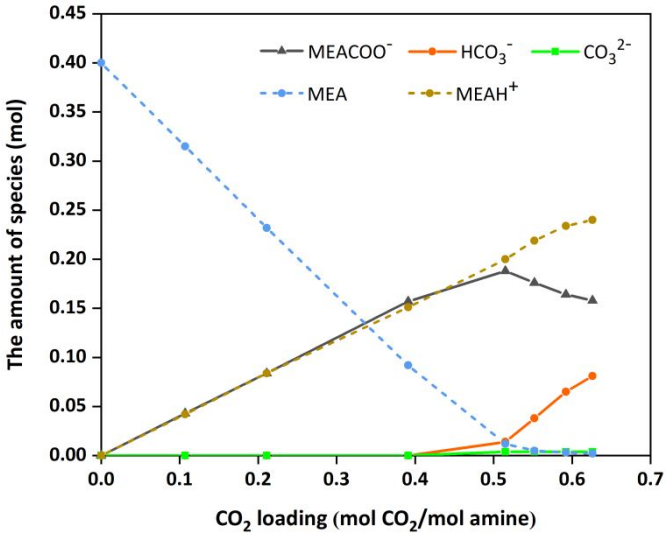

Figure 9. ^{13}C NMR speciation analysis as a function of the CO_2 loading.

Subsequently, a large amount of heat is still required for continuous CO_2 desorption from $MEACOO^-$ decomposition. However, catalysts can accelerate this process mainly due to Brønsted and Lewis acid sites on the catalyst surface [13, 19]. In this work, the SEP surface was modified with the metal oxides CuO and Fe_2O_3, which are able to act predominantly as Lewis acids due to the unsaturated metal atoms exist as it can accept the electron pair[39], so the metal oxide (CuO and Fe_2O_3) in this work is expected predominately act as a Lewis acidity. On the other hand, the SEP itself has different "kinds" of water (**Figure 1**) that could convert to hydroxyl group, which can subsequently provide the proton to bases such as HCO_3^- or $MEACOO^-$ to release CO_2: therefore, it can be concluded that the SEP can be regarded as a Brønsted acid site (donating protons).

The regeneration mechanism of CO_2-loaded aqueous MEA with SEP-based catalysts is shown in **Figure 10**, where M represents the unsaturated metal atoms on

the SEP-catalyst. Through a chemisorption process, the conjugated base (SEP-O^-) of Brønsted acid obtains the proton from $MEAH^+$ to release MEA; subsequently SEP-OH can transfer the proton onto the oxygen of $MEACOO^-$ (forming MEACOOH), then the proton moves from the O atom to the N atom through isomerization (forming the zwitterionic form $MEAH^+COO^-$). Meanwhile, Lewis acid accepts the lone electron pairs on the O and N atoms of $MEAH^+COO^-$, then stretches the C-N bond to facilitate its decomposition, resulting in the release of MEA and CO_2. This catalyst-assisted proton transfer process, due to the synergistic work of the Brønsted and Lewis acid sites, facilitates the $MEAH^+$ deprotonation and the $MEACOO^-$ decomposition, lowering their activation energies, thus allowing the CO_2 desorption with a lower energy input, in agreement with the obtained results shown in **Figure 3**.

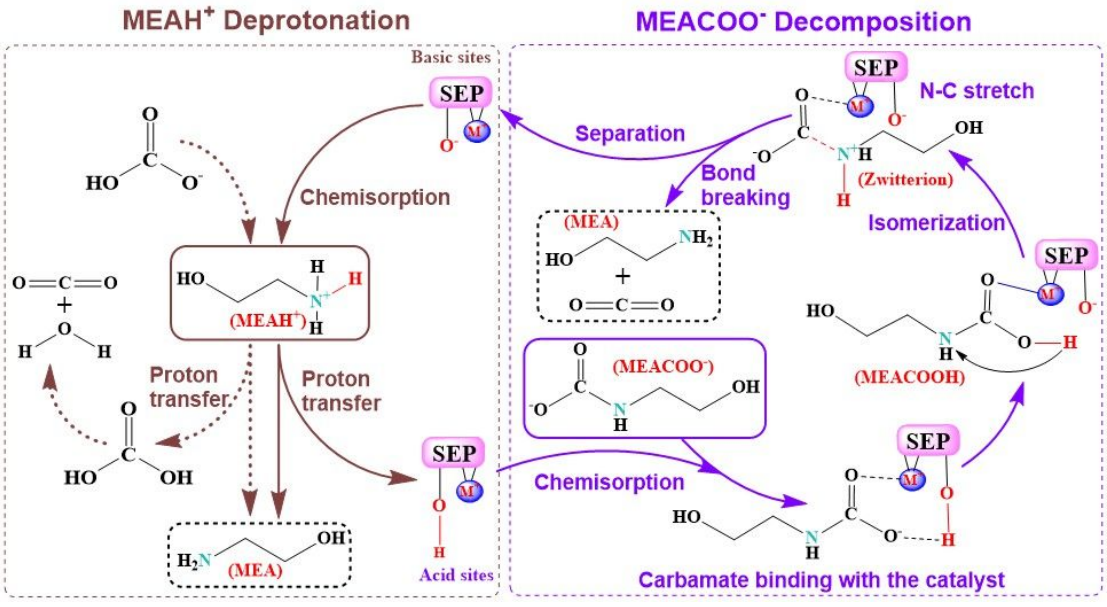

Figure 10. The pathways of $MEAH^+$ deprotonation and $MEACOO^-$ decomposition in the catalyst-aided desorption process for MEA.

Stability evaluation of the catalyst

High stability is a very important property for catalysts which determines the recycling efficiency for solvent regeneration, especially in industrial-scale applications. In this work, the Fe_2O_3-SEP catalyst was used for six consecutive catalytic desorption experiments with CO_2-loaded MEA solutions to verify its stability over time under the operating conditions used, the results of these recycling tests are shown in **Figure 11**, compared with desorption results obtained without catalyst (blank). The change in CO_2 loading as a function of desorption time is shown in **Figure 11a**, which clearly shows that all processes conducted with the Fe_2O_3-SEP catalyst, even after six reuses, decreased the residual amount of CO_2 in solution more rapidly than the blank. **Figure 11b** shows that the Fe_2O_3-SEP catalyst maintains high catalytic activity, with no significant decay effect, even after six consecutive uses. Fresh Fe_2O_3-SEP (1st) reduced the energy consumption for CO_2 desorption to 52.8% compared to the MEA solution without catalyst, while after the catalyst was recycled six times (6th), the energy consumption for CO_2 desorption was still reduced to 56.8%, which is only 4.0% higher than the first time. In addition, **Figure 11b** also displays that the amount of desorbed CO_2 is almost the same for all cycles: 0.136 mol of CO_2 was released with the fresh catalyst, and 0.120 mol of CO_2 can still be desorbed at the sixth reuse. Meanwhile, the average CO_2 desorption rate decreases from 68 to 59.8 after the 6 cyclic tests, which means that less CO_2 is released with a slower desorption rate when cyclically using the catalyst, which leads to increased heat consumption. In summary, after six successive reuses, the Fe_2O_3-SEP catalyst still has an acceptable catalytic efficiency for CO_2

desorption. The reduced energy consumption can significantly save the operating cost for post-combustion CO_2 capture.

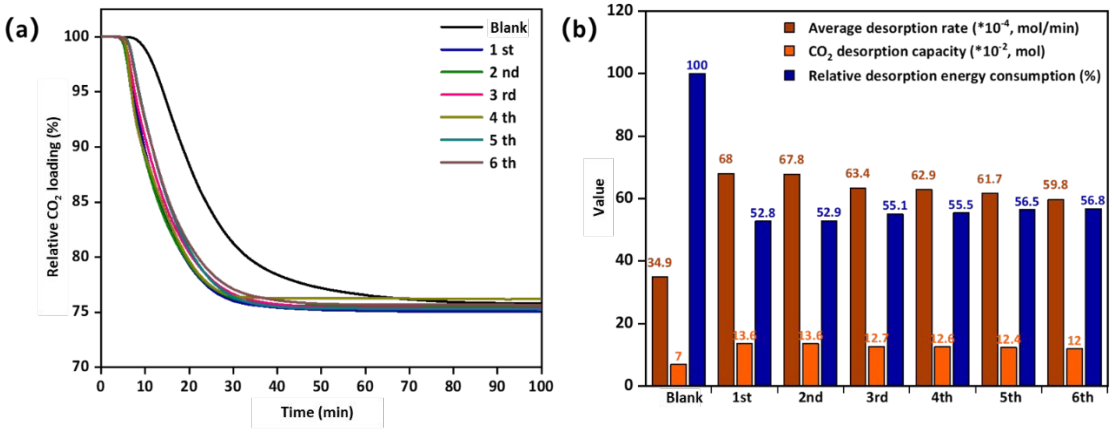

Figure 11. Cyclic stability test of the Fe_2O_3-SEP catalyst, including (a) relative CO_2 loading changing curves and (b) catalytic CO_2 desorption performance.

■ Conclusions

In this work, the low-cost environmentally friendly sepiolite (SEP) was selected as an efficient catalyst carrier, and two metal oxide catalysts supported by SEP (Fe_2O_3-SEP and CuO-SEP) were synthesized by the impregnation method. Analysis of the catalytic CO_2 desorption performances of SEP, Fe_2O_3-SEP and CuO-SEP in MEA solution led to the following conclusions:

(1) Compared with the blank experiment, the addition of catalysts can effectively reduce the energy consumption for CO_2 desorption, accelerate the CO_2 desorption rate, and increase the amount of the released CO_2. Among the tested catalysts, Fe_2O_3-SEP shows the best catalytic performance. The calculated relative desorption energy consumption (RH, %) decreased in the order: blank (100) > SEP (66.4) > CuO-SEP (58.8) > Fe_2O_3-SEP (54.0).

(2) The characterization of catalysts revealed that a large mesoporous specific surface area and more Brønsted acid sites enhance the catalytic CO_2 desorption performance.

(3) Stability tests conducted on Fe_2O_3-SEP catalyst demonstrated that its high performance in CO_2 desorption processes was maintained even at the sixth consecutive reuse. Overall, the metal oxide catalysts supported by SEP can effectively promote the CO_2 desorption at a lower temperature, thus reducing the desorption energy consumption for CO_2 capture process with amine-based solution. As the SEP is a clay type of material obtained from nature, it deserves to be further investigated and applied in industry as a green, environmentally friendly, and efficient catalyst carrier for catalytic CO_2 desorption.

Acknowledgement

The work was supported by National Natural Science Foundation of China (22008204), The China Postdoctoral Science Foundation (2021M692704), and Research Start-up Foundation of Xiangtan University (21QDZ56).

References

1. Bui, M.; Adjiman, C. S.; Bardow, A.; Anthony, E. J.; Boston, A.; Brown, S.; Fennell, P. S.; Fuss, S.; Galindo, A.; Hackett, L. A., Carbon capture and storage (CCS): the way forward. *Energy & Environmental Science* **2018,** 11, (5), 1062-1176. DOI: 10.1039/C7EE02342A

2. Liu, H.; Jiang, X.; Idem, R.; Dong, S.; Tontiwachwuthikul, P., AI models for correlation of physical properties in system of 1DMA2P-CO2-H2O. *AIChE Journal* **2022,** 68, (9), e17761. DOI: 10.1002/aic.17761

3. Liang, Z. H.; Rongwong, W.; Liu, H.; Fu, K.; Gao, H.; Cao, F.; Zhang, R.; Sema, T.; Henni, A.; Sumon, K., Recent progress and new developments in post-combustion carbon-capture technology with amine based solvents. *International Journal of Greenhouse Gas Control* **2015,** 40, 26-54. DOI: 10.1016/j.ijggc.2015.06.017

4. He, X.; He, H.; Barzagli, F.; Amer, M. W.; Li, C. e.; Zhang, R., Analysis of the energy consumption in solvent regeneration processes using binary amine blends for CO2 capture. *Energy* **2023,** 270, 126903. DOI: 10.1016/j.energy.2023.126903

5. Yu, Y.; Shen, Y.; Zhou, X.; Liu, F.; Zhang, S.; Lu, S.; Ye, J.; Li, S.; Chen, J.; Li, W., Relationship between tertiary amine's physical property and biphasic solvent's CO2 absorption performance: Quantum calculation and experimental demonstration. *Chemical Engineering Journal* **2022,** 428, 131241. DOI: 10.1016/j.cej.2021.131241

6. Shen, Y.; Liu, F.; Wang, X.; Shao, P.; He, Z.; Zhang, S.; Chen, L.; Li, S.; Li, W.; Wang, L.; Hou, Y., A pore matching amine-functionalized strategy for efficient CO2 physisorption with low energy penalty. *Chemical Engineering Journal* **2022,** 432, 134403. DOI: 10.1016/j.cej.2021.134403

7. Wang, L.; Zhang, Y.; Wang, R.; Li, Q.; Zhang, S.; Li, M.; Liu, J.; Chen, B., Advanced Monoethanolamine Absorption Using Sulfolane as a Phase Splitter for CO2 Capture. *Environmental Science & Technology* **2018,** 52, (24), 14556-14563. DOI: 10.1021/acs.est.8b05654

8. Shao, P.; He, Z.; Hu, Y.; Shen, Y.; Zhang, S.; Yu, Y., Zeolitic imidazolate frameworks with different organic ligands as carriers for Carbonic anhydrase immobilization to promote the absorption of CO2 into tertiary amine solution. *Chemical Engineering Journal* **2022,** 435, 134957. DOI: 10.1016/j.cej.2022.134957

9. Dong, S.; Quan, H.; Zhao, D.; Li, H.; Geng, J.; Liu, H., Generic AI models for mass transfer coefficient prediction in amine-based CO2 absorber, Part I: BPNN model. *Chemical Engineering Science* **2022,** 264, 118165. DOI: 10.1016/j.ces.2022.118165

10. Quan, H.; Dong, S.; Zhao, D.; Li, H.; Geng, J.; Liu, H., Generic AI models for mass transfer coefficient prediction in amine-based CO2 absorber, Part II: RBFNN and RF model. *AIChE Journal* **2022,** n/a, (n/a), e17904. DOI: 10.1002/aic.17904

11. Chen, G.; Chen, G.; Peruzzini, M.; Barzagli, F.; Zhang, R., Investigating the Performance of Ethanolamine and Benzylamine Blends as Promising Sorbents for Postcombustion CO2 Capture through 13C NMR Speciation and Heat of CO2 Absorption Analysis. *Energy & Fuels* **2022,** 36, (16), 9203-9212. DOI: 10.1021/acs.energyfuels.2c01930

12. Zhang, R.; Zhang, X.; Yang, Q.; Yu, H.; Liang, Z.; Luo, X., Analysis of the reduction of energy cost by using MEA-MDEA-PZ solvent for post-combustion carbon dioxide capture (PCC). *Applied Energy* **2017,** 205, 1002-1011. DOI: 10.1016/j.apenergy.2017.08.130

13. Tan, Z.; Zhang, S.; Yue, X.; Zhao, F.; Xi, F.; Yan, D.; Ling, H.; Zhang, R.; Tang, F.; You, K.; Luo, H. a.; Zhang, X., Attapulgite as a cost-effective catalyst for low-energy consumption amine-based CO2 capture. *Separation and Purification Technology* **2022,** 298, 121577. DOI: 10.1016/j.seppur.2022.121577

14. Alivand, M. S.; Mazaheri, O.; Wu, Y.; Stevens, G. W.; Scholes, C. A.; Mumford, K. A., Catalytic Solvent Regeneration for Energy-Efficient CO2 Capture. *ACS Sustainable Chemistry & Engineering* **2020,** 8, (51), 18755-18788. DOI: 10.1021/acssuschemeng.0c07066

15. de Meyer, F.; Bignaud, C., The use of catalysis for faster CO2 absorption and energy-efficient solvent regeneration: An industry-focused critical review. *Chemical Engineering Journal* **2022,** 428, 131264. DOI: 10.1016/j.cej.2021.131264

16. Xing, L.; Wei, K.; Li, Y.; Fang, Z.; Li, Q.; Qi, T.; An, S.; Zhang, S.; Wang, L., TiO2 Coating Strategy for Robust Catalysis of the Metal–Organic Framework toward Energy-Efficient CO2 Capture. *Environmental Science & Technology* **2021,** 55, (16), 11216-11224. DOI: 10.1021/acs.est.1c02452

17. Xing, L.; Li, M.; Li, M.; Xu, T.; Li, Y.; Qi, T.; Li, H.; Hu, Z.; Hao, G.-p.; Zhang, S.; James, T. D.; Mao, B.; Wang, L., MOF-Derived Robust and Synergetic Acid Sites Inducing C–N Bond Disruption for Energy-Efficient CO2 Desorption.

Environmental Science & Technology **2022,** 56, (24), 17936-17945. DOI: 10.1021/acs.est.2c06842

18. Li, T.; Yu, Q.; Barzagli, F.; Li, C. e.; Che, M.; Zhang, Z.; Zhang, R., Energy efficient catalytic CO2 desorption: mechanism, technological progress and perspective. *Carbon Capture Science & Technology* **2023,** 6, 100099. DOI: 10.1016/j.ccst.2023.100099

19. Zhang, R.; Li, T.; Zhang, Y.; Ha, J.; Xiao, Y.; Li, C. e.; Zhang, X.; Luo, H. a., CuO modified KIT-6 as a high-efficiency catalyst for energy-efficient amine solvent regeneration. *Separation and Purification Technology* **2022**, 121702. DOI: 10.1016/j.seppur.2022.121702

20. Liu, F.; Huang, K.; Zheng, A.; Xiao, F.-S.; Dai, S., Hydrophobic Solid Acids and Their Catalytic Applications in Green and Sustainable Chemistry. *ACS Catalysis* **2018,** 8, (1), 372-391. DOI: 10.1021/acscatal.7b03369

21. Liang, Z.; Idem, R.; Tontiwachwuthikul, P.; Yu, F.; Liu, H.; Rongwong, W., Experimental study on the solvent regeneration of a CO2 - loaded MEA solution using single and hybrid solid acid catalysts. *AIChE Journal* **2016,** 62, (3), 753-765. DOI: 10.1002/aic.15073

22. Bhatti, U. H.; Ienco, A.; Peruzzini, M.; Barzagli, F., Unraveling the Role of Metal Oxide Catalysts in the CO2 Desorption Process from Nonaqueous Sorbents: An Experimental Study Carried out with 13C NMR. *ACS Sustainable Chemistry & Engineering* **2021,** 9, (46), 15419-15426. DOI: 10.1021/acssuschemeng.1c04026

23. Zhang, X.; Zhang, X.; Liu, H.; Li, W.; Xiao, M.; Gao, H.; Liang, Z., Reduction of energy requirement of CO 2 desorption from a rich CO 2-loaded MEA solution by using solid acid catalysts. *Applied Energy* **2017,** 202, 673-684. DOI: 10.1016/j.apenergy.2017.05.135

24. Xing, L.; Wei, K.; Li, Q.; Wang, R.; Zhang, S.; Wang, L., One-Step Synthesized SO42–/ZrO2-HZSM-5 Solid Acid Catalyst for Carbamate Decomposition in CO2 Capture. *Environmental Science & Technology* **2020,** 54, (21), 13944-13952. DOI: 10.1021/acs.est.0c04946

25. Gao, H.; Huang, Y.; Zhang, X.; Bairq, Z. A. S.; Huang, Y.; Tontiwachwuthikul, P.; Liang, Z., Catalytic performance and mechanism of SO42−/ZrO2/SBA-15 catalyst for CO2 desorption in CO2-loaded monoethanolamine solution. *Applied Energy* **2020,** 259, 114179. DOI: 10.1016/j.apenergy.2019.114179

26. Zhang, X.; Zhu, Z.; Sun, X.; Yang, J.; Gao, H.; Huang, Y.; Luo, X.; Liang, Z.; Tontiwachwuthikul, P., Reducing Energy Penalty of CO2 Capture Using Fe Promoted SO42–/ZrO2/MCM-41 Catalyst. *Environmental Science & Technology* **2019,** 53, (10), 6094-6102. DOI: 10.1021/acs.est.9b01901

27. Ali Saleh Bairq, Z.; Gao, H.; Huang, Y.; Zhang, H.; Liang, Z., Enhancing CO2 desorption performance in rich MEA solution by addition of SO42−/ZrO2/SiO2 bifunctional catalyst. *Applied Energy* **2019,** 252, 113440. DOI: 10.1016/j.apenergy.2019.113440

28. Zhang, X.; Hong, J.; Liu, H.; Luo, X.; Olson, W.; Tontiwachwuthikul, P.; Liang, Z., SO42−/ZrO2 supported on γ-Al2O3 as a catalyst for CO2 desorption from CO2-loaded monoethanolamine solutions. *AIChE Journal* **2018,** 64, (11), 3988-4001. DOI: 10.1002/aic.16380

29. Nagendrappa, G., Organic synthesis using clay and clay-supported catalysts. *Applied Clay Science* **2011,** 53, (2), 106-138. DOI: 10.1016/j.clay.2010.09.016

30. Jha, A.; Garade, A. C.; Shirai, M.; Rode, C. V., Metal cation-exchanged montmorillonite clay as catalysts for hydroxyalkylation reaction. *Applied Clay Science* **2013,** 74, 141-146. DOI: 10.1016/j.clay.2012.10.005

31. Bhatti, U. H.; Sultan, H.; Min, G. H.; Nam, S. C.; Baek, I. H., Ion-exchanged montmorillonite as simple and effective catalysts for efficient CO2 capture. *Chemical Engineering Journal* **2021,** 413, 127476. DOI: 10.1016/j.cej.2020.127476

32. Bhatti, U. H.; Kazmi, W. W.; Muhammad, H. A.; Min, G. H.; Nam, S. C.; Baek, I. H., Practical and inexpensive acid-activated montmorillonite catalysts for energy-efficient CO2 capture. *Green Chemistry* **2020,** 22, (19), 6328-6333. DOI: 10.1039/D0GC01887B

33. Bhatti, U. H.; Kazmi, W. W.; Min, G. H.; Haider, J.; Nam, S.; Baek, I. H., Facilely Synthesized M-Montmorillonite (M = Cr, Fe, and Co) as Efficient Catalysts for Enhancing CO2 Desorption from Amine Solution. *Industrial & Engineering Chemistry Research* **2021,** 60, (36), 13318-13325. DOI: 10.1021/acs.iecr.1c02487

34. Tan, Z.; Zhang, S.; Zhao, F.; Zhang, R.; Tang, F.; You, K.; Luo, H. a.; Zhang, X., SnO2/ATP catalyst enabling energy-efficient and green amine-based CO2 capture. *Chemical Engineering Journal* **2023,** 453, 139801. DOI: 10.1016/j.cej.2022.139801

35. Choudhury, A.; Bhowmick, A. K.; Ong, C.; Soddemann, M., Influence of molecular parameters on thermal, mechanical, and dynamic mechanical properties of hydrogenated nitrile rubber and its nanocomposites. *Polymer Engineering & Science* **2010,** 50, (7), 1389-1399. DOI: 10.1002/pen.21680

36. Chivrac, F.; Pollet, E.; Schmutz, M.; Avérous, L., Starch nano-biocomposites based on needle-like sepiolite clays. *Carbohydrate Polymers* **2010,** 80, (1), 145-153. DOI: 10.1016/j.carbpol.2009.11.004

37. Galan, E.; Carretero, M. I., A New Approach to Compositional Limits for Sepiolite and Palygorskite. *Clays and Clay Minerals* **1999,** 47, (4), 399-409. DOI: 10.1346/CCMN.1999.0470402

38. Mohd Zaini, N. A.; Ismail, H.; Rusli, A., Short Review on Sepiolite-Filled Polymer Nanocomposites. *Polymer-Plastics Technology and Engineering* **2017,** 56, (15), 1665-1679. DOI: 10.1080/03602559.2017.1289395

39. Bhatti, U. H.; Shah, A. K.; Kim, J. N.; You, J. K.; Choi, S. H.; Lim, D. H.; Nam, S.; Park, Y. H.; Baek, I. H., Effects of Transition Metal Oxide Catalysts on MEA Solvent Regeneration for the Post-Combustion Carbon Capture Process. *ACS Sustainable Chemistry & Engineering* **2017,** 5, (7), 5862-5868. DOI: 10.1021/acssuschemeng.7b00604

40. Bhatti, U. H.; Nam, S.; Park, S.; Baek, I. H., Performance and Mechanism of Metal Oxide Catalyst-Aided Amine Solvent Regeneration. *ACS Sustainable Chemistry & Engineering* **2018,** 6, (9), 12079-12087. DOI: 10.1021/acssuschemeng.8b02422

41. Zhang, R.; Zhang, Y.; Cheng, Y.; Yu, Q.; Luo, X.; Li, C. e.; Li, J.; Zeng, Z.; Liu, Y.; Jiang, X.; Hu, X. E., New Approach with Universal Applicability for Evaluating the Heat Requirements in the Solvent Regeneration Process for Postcombustion CO2 Capture. *Industrial & Engineering Chemistry Research* **2020,** 59, (7), 3261-3268. DOI: 10.1021/acs.iecr.9b05247

42. Barzagli, F.; Peruzzini, M.; Zhang, R., Direct CO2 capture from air with aqueous and nonaqueous diamine solutions: a comparative investigation based on 13C NMR analysis. *Carbon Capture Science & Technology* **2022,** 3, 100049. DOI: 10.1016/j.ccst.2022.100049

43. Shi, H.; Naami, A.; Idem, R.; Tontiwachwuthikul, P., Catalytic and non catalytic solvent regeneration during absorption-based CO_2 capture with single and blended reactive amine solvents. *International Journal of Greenhouse Gas Control* **2014,** 26, 39-50. DOI: 10.1016/j.ijggc.2014.04.007

44. Sun, Q.; Li, T.; Mao, Y.; Gao, H.; Sema, T.; Wang, S.; Liu, L.; Liang, Z., Reducing Heat Duty of MEA Regeneration Using a Sulfonic Acid-Functionalized Mesoporous MCM-41 Catalyst. *Industrial & Engineering Chemistry Research* **2021,** 60, (50), 18304-18315. DOI: 10.1021/acs.iecr.1c03671

45. Bhatti, U. H.; Shah, A. K.; Hussain, A.; Khan, H. A.; Park, C. Y.; Nam, S. C.; Baek, I. H., Catalytic activity of facilely synthesized mesoporous HZSM-5 catalysts for optimizing the CO2 desorption rate from CO2-rich amine solutions. *Chemical Engineering Journal* **2020,** 389, 123439. DOI: 10.1016/j.cej.2019.123439

46. Zhang, X.; Huang, Y.; Gao, H.; Luo, X.; Liang, Z.; Tontiwachwuthikul, P., Zeolite catalyst-aided tri-solvent blend amine regeneration: An alternative pathway to reduce the energy consumption in amine-based CO2 capture process. *Applied Energy* **2019,** 240, 827-841. DOI: 10.1016/j.apenergy.2019.02.089

47. Zhang, X.; Liu, H.; Liang, Z.; Idem, R.; Tontiwachwuthikul, P.; Jaber Al-Marri, M.; Benamor, A., Reducing energy consumption of CO2 desorption in CO2-loaded aqueous amine solution using Al2O3/HZSM-5 bifunctional catalysts. *Applied Energy* **2018,** 229, 562-576. DOI: 10.1016/j.apenergy.2018.07.035

48. Ali Saleh Bairq, Z.; Gao, H.; Murshed, F. A. M.; Tontiwachwuthikul, P.; Liang, Z., Modified Heterogeneous Catalyst-Aided Regeneration of CO2 Capture Amines: A Promising Perspective for a Drastic Reduction in Energy Consumption. *ACS Sustainable Chemistry & Engineering* **2020,** 8, (25), 9526-9536. DOI: 10.1021/acssuschemeng.0c02582

49. Wei, K.; Xing, L.; Li, Y.; Xu, T.; Li, Q.; Wang, L., Heteropolyacid modified Cerium-based MOFs catalyst for amine solution regeneration in CO2 capture. *Separation and Purification Technology* **2022,** 293, 121144. DOI: 10.1016/j.seppur.2022.121144

50. Ye, Q.; Yan, L.; Wang, H.; Cheng, S.; Wang, D.; Kang, T.; Dai, H., Enhanced catalytic performance of rare earth-doped Cu/H-Sep for the selective catalytic reduction of NO with C3H6. *Applied Catalysis A: General* **2012,** 431-432, 42-48. DOI: 10.1016/j.apcata.2012.04.014

51. Cho, J. M.; Han, G. Y.; Jeong, H.-K.; Roh, H.-S.; Bae, J. W., Effects of ordered mesoporous bimodal structures of Fe/KIT-6 for CO hydrogenation activity to hydrocarbons. *Chemical Engineering Journal* **2018,** 354, 197-207. DOI: 10.1016/j.cej.2018.07.205

52. Xia, Y.; Dai, H.; Jiang, H.; Zhang, L.; Deng, J.; Liu, Y., Three-dimensionally ordered and wormhole-like mesoporous iron oxide catalysts highly active for the oxidation of acetone and methanol. *Journal of Hazardous Materials* **2011,** 186, (1), 84-91. DOI: 10.1016/j.jhazmat.2010.10.073

53. Subhan, F.; Aslam, S.; Yan, Z.; Ikram, M.; Rehman, S., Enhanced desulfurization characteristics of Cu-KIT-6 for thiophene. *Microporous and Mesoporous Materials* **2014,** 199, 108-116. DOI: 10.1016/j.micromeso.2014.08.018

54. Alkan, M.; Tekin, G.; Namli, H., FTIR and zeta potential measurements of sepiolite treated with some organosilanes. *Microporous and Mesoporous Materials* **2005,** 84, (1), 75-83. DOI: 10.1016/j.micromeso.2005.05.016

55. Gao, Y.; Gan, H.; Zhang, G.; Guo, Y., Visible light assisted Fenton-like degradation of rhodamine B and 4-nitrophenol solutions with a stable poly-hydroxyl-iron/sepiolite catalyst. *Chemical Engineering Journal* **2013,** 217, 221-230. DOI: 10.1016/j.cej.2012.11.115

56. Caplow, M., Kinetics of carbamate formation and breakdown. *Journal of the American Chemical Society* **1968,** 90, (24), 6795-6803. DOI: 10.1021/ja01026a041

57. Hu, X. E.; Yu, Q.; Barzagli, F.; Li, C. e.; Fan, M.; Gasem, K. A. M.; Zhang, X.; Shiko, E.; Tian, M.; Luo, X.; Zeng, Z.; Liu, Y.; Zhang, R., NMR Techniques and Prediction Models for the Analysis of Species Formed in CO2 Capture Processes with Amine-Based Sorbents: A Critical Review. *ACS Sustainable Chemistry & Engineering* **2020,** 8, (16), 6173-6193. DOI: 10.1021/acssuschemeng.9b07823

58. Chen, G.; Chen, G.; Peruzzini, M.; Zhang, R.; Barzagli, F., Understanding the potential benefits of blended ternary amine systems for CO2 capture processes through 13C NMR speciation study and energy cost analysis. *Separation and Purification Technology* **2022,** 291, 120939. DOI: 10.1016/j.seppur.2022.120939

59. Zhang, R.; Liang, Z.; Liu, H.; Rongwong, W.; Luo, X.; Idem, R.; Yang, Q., Study of Formation of Bicarbonate Ions in CO2-Loaded Aqueous Single 1DMA2P and MDEA Tertiary Amines and Blended MEA–1DMA2P and MEA–MDEA Amines for Low Heat of Regeneration. *Industrial & Engineering Chemistry Research* **2016,** 55, (12), 3710-3717. DOI: 10.1021/acs.iecr.5b03097

738 For Table of Contents Use Only

739